Original Article: A review of Investigation of the Formation Kinetics of TBAC-like Clathrate Dual Hydrates

Alireza Bozorgian*

Department of Chemical Engineering, Mahshahr Branch, Islamic Azad University, Mahshahr, Iran

Use yor device to scan and read the article online

Citation A. Bozorgian* **A review of Investigation of the Formation Kinetics of TBAC-like Clathrate Dual Hydrates**. *J. Chem. Rev.*, **2021**, *3*(2), 109-120.

https://doi.org/10.22034/JCR.2021.278639.1106

Article info:
Received: 27 March 2021
Accepted: 20 May 2021
Available Online: 20 May 2021
ID: JCR-2103-1106
Checked for Plagiarism: Yes
Language Editor:
Mr. Ermia Aghaie
Editor who Approved Publication:
Prof. Dr. Ghasem Rezanejade Bardajee

Keywords:
Hydrate formation; TBAC-Like; Water network; Clarite; Chemical interaction

ABSTRACT

In this work a review of the formation kinetics of TBAC-like clathrate dual hydrates is discussed. Natural gas hydrate is a solid crystalline compound formed from a combination of water and gas, and these compounds are formed at low temperatures and relatively high pressures. Hydrate is a member of the clathrite family. The guest gas molecules are trapped inside the cavities of the water network (host), which is formed by hydrogen bonding between the molecules of the water molecule. Also, a clear example of which is smaller compounds than pentane in natural gas such as methane, ethane, propane and carbon dioxide can be formed by pure gas or a gas mixture consisting of two or more components. Clarite is considered to be a solid solution in which guest gas molecules and hydrate gases are in contact. The researchers are located with the host lattice (water), so gaseous hydrate is known as a non-stoichiometric solid, there is a strong hydrogen bond between the water molecules in the hydrate structure, while there is no chemical interaction between the guest and host molecules alone.

Introduction

General formula for gas hydrates is MnH2O, where M represents the guest molecule. An example of how gas molecules are trapped inside hydrate cavities, as shown in Figure 1 [1-4].

History of Natural Gas Hydrate is Dvided into Three Main Periods

Period 1: This period began with the discovery of Humphrey Davy in 1810 and continues to this day, and is related to the phenomenon of hydrate formation from a scientific point of view. Because the accumulation of water and gas in a solid phase (hydrate) is a scientifically significant phenomenon [6-8]

Period 2: Almost from 1934 after the discovery of Schmidt, stating that the formation of hydrates causes the closure of natural gas

***Corresponding Author:** *Alireza Bozorgian (a.bozorgian@mhriau.ac.ir),*

transmission lines began and continues to this day. Dayton and Frost were the first to perform experimental experiments on hydrate formation conditions and report data from it. During this period, hydrate is mainly considered as a problem for natural gas producers and processors. In other words, in this part of the history of hydrate, it is dedicated to the construction of industries and the problems caused by it [9-11]

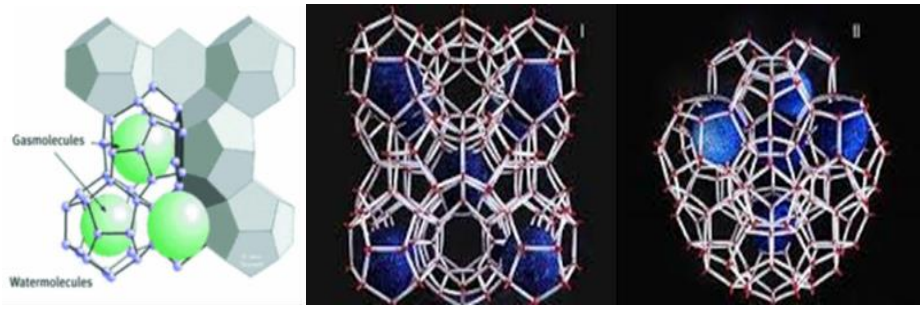

Figure 1. Trapping of guest gas molecules inside water cavities [5].

Third Dynasty: This period began in the mid-1970s with the discovery that nature produced hydrates millions of years before humans and continues to this day [12-14] These hydrates are found in glacial regions of the deep oceans as well as in the deep oceans as well as outside the Earth's atmosphere on other planets such as Mars. [15-17]. In 1950, the structure of the hydrate crystal lattice was examined by X-rays. This led to the development of the idea of using statistical thermodynamics to justify and interpret conditions. The emergence of these crystals. In the 1960s, it was discovered that large numbers of these molecules were present in the subterranean layers, which also contain a large amount of natural gas [18].

This huge volume of gas trapped in the hydrate crystal led many people to invent new methods or improve existing methods to extract these trapped gases. During the years 1960 to 1970, activities for desalination and desalination of seawater using hydrate formation were performed and the possibility of this work was shown in semi-industrial units, but at that time, due to lack of economic justification, it did not reach the design and production stage [19-22].

Since 1996, with the growing tendency to use hydrates in the separation and transfer of natural gas, research work on the use of thermodynamic and kinetic enhancers in the hydration process has intensified [23].

Structure of Gaseous Hydrates

Hydrate structure contains 85% water. Therefore, many of its mechanical properties are similar to ice. The structural properties of the hydrate crystal lattice were first studied by Müller. From the building, three types of hydrates named 1, 2 and 3 have been identified for hydrates so far. Structures 1 and 2 both have cubic structures [24-26]. Prior to the discovery of another building known as Building 3, it was thought that molecules larger than normal butane, due to their large size, could not be placed in the space created in the hydrate crystal lattice [27-29].

By discovering type 3 hydrate crystals, Rip mister has shown that molecules such as methyl cyclohexane, along with other small gaseous molecules such as methane or hydrogen sulfide, which are called auxiliary gases, can also produce type H hydrate crystals [30-33].

Depending on the type of gas that is placed in the empty space of the network, the geometric shape of the hydrate changes. The simplest idea of building a hydrate network is to place a ball inside a cage. If the ball is too small, the ball will come out. If the ball is too large, the cage will break; otherwise, it will remain in the cage. [34-37] For each hydrate structure network unit, there are several types of cages: S-type cage (small cage), M-type cage (medium cage) and L-type cage (large cage) [38-41]. The network unit of structure I consists of a 12A° cube, and the

general formula for hydrate is 8G + 46H2O, meaning that 46 molecules of water can form 8 cavities. It consists of two holes S (512) and six holes L (51262). 512 means a hole with 12 pentagonal plates and 51262 means a hole with 2 hexagonal plates and 12 pentagonal plates [42-45]. The network unit of structure II consists of a cube A˚ 3 / 17 that each building unit consists of 136 water molecules and 24 holes for gas molecules. 16 holes S (512) and 8 holes L (51264) [4] network structure unit H Which Each building unit consists of 34 water molecules and 6 holes for gas molecules. Three holes are of type S (512), two holes are of type M (435663) and one hole is type L (51268).

Conditions for Hydrate Formation

The conditions under which gaseous hydrates can be formed are

Preliminary Conditions

A: Existence of water in liquid or ice phase.

B: The presence of non-polar or slightly polar gas molecules of appropriate size.

C: High pressures and low temperatures [46].

Secondary Conditions

A: High gas flow velocities

B: Pressure fluctuations

C: Formation of a small hydrate crystal [47]

Applications of gaseous hydrates

Hydrates were first recognized as a factor in the obstruction of gas pipelines, but today many studies have been done on these compounds and have found various applications [47-49].

Absorption of carbon dioxide from the air

Because carbon dioxide is a greenhouse gas that causes global warming, its separation and storage is an environmental issue. A 64% increase in greenhouse gas emissions is due to carbon dioxide emissions. One way to reduce carbon dioxide is to separate it from the environment and introduce it into the depths of the seas and oceans [50-55] At depths below 400 meters, carbon dioxide gas is injected and dissolved in water to Falls into the trap. At a distance of 100-2000 meters, carbon dioxide is in a liquid state and penetrates into the water. Carbon dioxide hydrate is formed in 500-900 m of seawater [56-59].

The process of separation from the gas mixture

Separation by formation of gaseous hydrates is a new method. Reasons for using hydrates in separation processes include:

- Hydrate crystals are made up of only guest molecules and water [60]
- Each gas molecule as a guest molecule cannot be included in the structure of hydrate crystals and only certain molecules due to their chemical nature, shape and size can participate in the structure of hydrate [61-65].

When hydrate is formed in a gas mixture, the hydrate phase will be rich in gas, which is more inclined to form hydrate, and the remaining gas phase will be enriched with other gases [65-69]. Based on this argument, the hydrate formation process can be used to separate gases, especially when the use of conventional separation processes such as distillation is not possible, such as systems that have close boiling points and have high separation rates at separation costs [70-72].

Other applications of hydrate in the separation process include

- It separates CO2 from combustible gaseous mixtures.
- Another process called hydrate separation (HBGS) involves tetrahydrofuran (THF), which is used as a precursor to hydrate formation. THF lowers the equilibrium pressure of hydrate formation and expands the hydrate stability zone. The HBGS process allows the recovery of 99 mol% of CO2 from combustion gases at normal temperature K (283-273) [73-75].
- Separation is ethylene from the mixture and ethylene in the presence (SDS) and without SDS [76].
- Concentrate solutions by forming hydrates.
- Seawater desalination [77].

Natural gas storage and transmission

In recent years, the use of gas hydrates for storage and transmission of natural gas, especially for small and remote gas fields has been proposed. About 3% of the world's natural gas fields are small and medium-sized fields, half of which are remote fields. The energy density of methane hydrate is equal to the energy density of compressed gas but less than the energy density of liquefied petroleum gas (LNG) for which conventional methods such as LNG are not economically justified.

Natural gas hydrate is a suitable option for gas transfer [78]. The self-retaining properties of the hydrate allow the hydrate to remain stable at pressures below its formation pressure. In this case, if it does not reach that heat, the hydrate will not decompose. In fact, part of the surface of the hydrate decomposes and the resulting water freezes and covers it like a protective layer, preventing further decomposition [79-81].

One of the advantages of the hydrate method is that it does not require very low temperatures such as the required temperature of LNG or very high pressures such as the required pressure of CNG and its production process is short and it can be used in the sea and in the place of wells on the platform. There are between 150 and 180 volumes of gas in each volume of hydrates under standard conditions, and according to economic estimates, the cost of a gas-hydrate cycle is 25% less than has been LNG. The main problems of this process are low conversion rate, low speed and difficulty in separating excess water. It seems that in the not-too-distant future, the NGH process can be used as a method for gas storage and transport [82].

Cooling tanks

One of the applications of hydrate-containing slurries is to create a cold in the cooling cycle. These materials decompose by absorbing energy from the environment and cause it to cool. One of the positive points of this process is its compatibility with the environment [83-85].

Effect of additives on hydrate formation

In general, additives used in the formation of hydrates can be divided into two general categories: inhibitors and enhancers [86-88].

Inhibitors such as: methanol, ethanol, monoethylene glycol (MEG), diethylene glycol (DEG), Triethylene glycol (TEG), low injection inhibitors (LDHI), anti-cumulative (AA), kinetic (KI) [6] which is injected to prevent hydrate formation in gas transmission lines.

Thermodynamic improvers advance the formation of gaseous hydrates towards formation at low pressures and high temperatures (optimal thermodynamic conditions) [89-92]. Kinetic improvers can be classified into two groups: surfactants and hydrotropes. Surfactants are the most important kinetic enhancers.

Surfactants are divided into several categories based on hydrophilic groups:

Anionic surfactants (sodium dodecyl sulfate is an example of anionic surfactants), cationic surfactants (tetracyltrimethylammonium), nonionic surfactants (polyoxyethylene nonyl ether) and dual ionic surfactants (Amino acids (nanoparticles) are another class of kinetic enhancers [93-95].

Thermodynamic improvers are divided into two general categories:

The first category of water-soluble materials and the second category of materials They are insoluble in water. The first class of these substances, which are easily soluble in water and are divided into two categories, saline compounds and non-saline compounds. Non-saline compounds usually form structure II. The most important of these compounds are tetrahydrofuran, 1 and 4-dioxane, acetone and furan. When gaseous hydrates are formed in the presence of such improvers, due to the large size of these compounds, they are placed in large cavities and the gas molecules occupy small particles. In this case, structure II hydrates are formed, which changes the thermodynamic conditions Water-insoluble improvers, depending on their molecular size, form two types of hydrate structures. Materials such as cyclobutane, cyclopentane, cyclohexane, etc. form structure II and compounds such as methylcyclohexane, methylcyclopentane, etc.,

which have a larger molecular size, form the H structure [96-99]

The structure of hydrates formed in the presence of water-soluble salt compounds differs from conventional hydrate structures. In addition to being located inside the cavities, these materials also participate in the structure of the hydrate network, which is why the hydrates formed in the presence of these materials are called quasi-clarities. These compounds significantly facilitate the formation of hydrates and are able to form hydrates in environmental conditions [100].

Clarite-like hydrates

One of the costliest steps in hydrate formation is the process of compressing gas to relatively high pressures, as well as the need for low temperatures to form hydrates. To solve this problem and facilitate the formation of hydrates, researchers have done a lot of research on thermodynamic facilitators. The use of thermodynamic facilitators results in the formation of dual hydrates [101].

Thus, these additives, together with the main hydrating gas, occupy the cavities of the hydrate crystal lattice. One of the best of these substances, which greatly facilitates the formation of hydrates, is THF. But the most important problem with this substance is that it is volatile and toxic. Therefore, it is very important to use substances that can facilitate the formation of hydrates and also do not have problems such as toxicity, volatility and flammability.

In 1940, new structures of hydrates were first discovered by Fuller et al. [5] The structural nature of the hydrates discovered differs from that of simple gaseous hydrates. In this type of hydrate, the guest molecules, in addition to being placed inside the hydrate cavities, also participate in the structure of the hydrate network. For this reason, these structures are called quasi-claritite. Because tetraalkylammonium salts produce clathrite-like hydrates, these hydrates are called ionic hydrates [6] Hydrate formation. Clarite-like hydrates are composed of tetra-n-butyl or tetra-ISO-amyl salts on the quaternary ammonium or phosphonium cation. The anions are attached to water molecules by hydrogen bonds to form part of the clathrite structure. Tetra n-butyl ammonium halide (TBAX) -like hydrate (TBAX) is stable at atmospheric pressure and temperature. Tetra-n-butyl ammonium bromide (TBAB), tetra-n-butyl ammonium chloride (TBAC) and tetra-n-butyl ammonium Fluoride (TBAF) are examples of these salts.

Tetra-n-butyl ammonium bromide, part of the structure of which is shown with the hydrate number 38 in Figure 1-4, has two 14-sided cavities of Tetra Kai Deca Hadron (51262), two 15-sided cavities of Penta Kai Deca Hadron (51263). And the two 12-sided cavities are the two deca hedron (512).

The 14- and 15-sided cavities are occupied by the tetra-n-butyl ammonium cation. Shimada et al. [44] Unoccupied cavities This structure is capable of being occupied by small molecules such as methane. Hydrogen, nitrogen and hydrogen sulfide are identified. The small 12-sided cavities (512) can be filled with water or gas molecules of the right size or left empty [100-102].

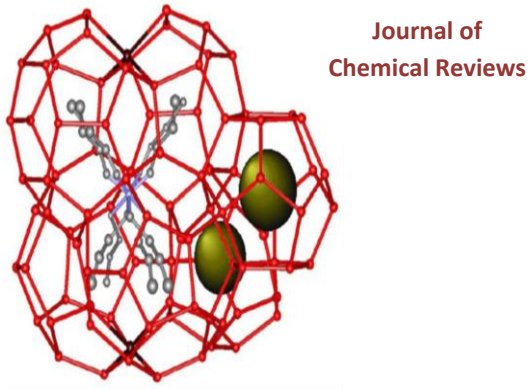

Figure 2. Structure [TBAB.38H2O32].

The most common structures of clathrite-like hydrates for tetra-butyl ammonium salts are Cube I (CSS-I), quadrilateral I (TS-I) and hexagonal I (HS-I) [1].

Three structures have been reported for TBAC clathrite hydrate:

TBAC.24H2O, TBAC.30H2O and [32] TBAC.32H2O. The stability of each of these structures depends on the TBAC concentration, temperature and pressure used.

TBAF-like clathrite hydrate has two known structures:

The CSS-I structure (TBAF.29 / 7H2O) and the TS-I structure (TBAF.H2O) [18].

An overview of the content done

Quantitative research has been done on the kinetics of methane gas hydrate formation in the presence of TBAC. In this chapter, we will discuss some kinetic and thermodynamic studies related to gas hydrate. At first, a brief description of the improvement method We express kinetic donor and thermodynamic enhancer.

In the kinetic enhancer of hydration formation, methods are used that can reduce the formation time of hydrate and increase its growth rate. Addition of surfactants are as follows [22]. Surfactants improve the properties of the system, for example, increase the solubility of non-polar gases in water.

The process of hydrate formation is also strongly influenced by surface forces, so surfactants can improve Conditions for hydrate formation. Of course, the effects of chemicals on hydrate formation also depend on the type of gaseous hydrate structure formed in the given system [55] SDS, which is an anionic surfactant and on the kinetic parameters of hydrate formation (such as induction time, Storage capacity, water to hydrate conversion rate and hydrate formation rate).

The thermodynamic method is in two ways:

1- Adding an improver to the water-gas system so that you can reduce the pressure of hydrate formation at the desired temperature.

2- Adding materials to the system that are capable of forming type H hydrates. Because the presence of these compounds causes the H type structure to be formed in the system instead of type I and II structures, because this structure provides more space for transferable gases and through this, a larger volume of gas will be transferred [96].

Abolfazl Mohammadi et al. Investigated the kinetics of carbon dioxide formation in the presence of silver nanoparticles and SDS. For this purpose, several solutions with concentrations of 300 and 500 PPM were prepared from SDS, and solutions with concentrations of M000045 and 0.00009 M were prepared from silver nanoparticles as well as a mixture of SDS and silver nanoparticles.

Experiments were performed at K temperatures (275.65 and 273.65) and at MPa cell inlet pressures. The results showed that SDS and silver nanoparticles did not have a significant effect on reducing the induction time and increasing the storage capacity of carbon dioxide. However, the mixture of SDS and silver nanoparticles has a significant effect on increasing carbon dioxide storage.

Analysis of hydrate growth rates at the beginning of hydrate formation showed that SDS and silver nanoparticles had a constant value of the apparent rate of hydrate growth at the time of induction and with increasing hydrate growth time the constant rate of apparent rate decreased and decreased by a small amount. Mixtures of SDS and silver nanoparticles have the highest initial rate of hydrate growth [78].

Zhang et al. Compared the formation of methane hydrate between a stirred reactor and a fixed bed of porous medium (silica granules) in the presence of sodium dodecyl sulfate (SDS). Experiments were performed at 7 MPa pressure and 274.15 K temperature. The concentration of SDS in the range (PPM1500-300) has been used. The results showed that the concentration of SDS in PPM500 is the optimal concentration for

the formation of methane hydrate and the formation of methane hydrate at a considerable rate in the fixed bed of silicon grains with The concentration of SDS, PPM 500, increases compared to those using SDS in an agitator reactor, the hydrated water and storage capacity are 78.1% and 139.8 V / V, respectively [39].

Hamid Ganji et al. Effects of anionic surfactants of sodium dodecyl sulfate (SDS) and linear sodium dodecyl benzene sulfonate (LABS), cationic surfactants of acetyl trim ethyl ammonium bromide (CTAB) and non-surfactants Ethoxylated nonylphenol (ENP) ions were investigated in the formation, decomposition and storage capacity of methane hydrate.

Each of the surfactants has three concentrations of PPM (300, 500, 1000) and it was found that SDS when prepared with these three concentrations significantly increases the rate of hydrate formation. LABS increases the rate of formation at concentrations of 500 and 1000 PPM but decreases at 300 PPM. CTAB and ENP have an improving effect on the rate of hydrate formation at 1000 PPM but decreases at concentrations of 300 and 500. Hydrate stability tests were performed at 268.2, 270.2 and 272.2 with and without surface improvers. The results showed that all tests in the presence of additives reduced the decomposition rate of methane hydrate to below [59]

CTAB had the least effect and LABS had the most effect on the decomposition rate of methane, and laboratory results in the volume of hydrate gas showed that the highest storage capacity was 165 V / V at a concentration of 1000 PPM of CTAB in water Obtained [63].

Engelzo et al. Studied the kinetics of methane and ethane gas hydration, and proposed an internal kinetic model with an adjustable parameter for methane and ethane hydration. Laboratory data were performed in an agitator reactor tank at four temperatures from K (274 to 282) and at a limited MPa pressure (0.636 to 8.903). The kinetic model is based on the crystallization theory, while the two-film model theory is adapted for surface mass transfer [67]

Experiments were performed at different agitator velocities to define the kinetic method. Studies have shown that the amount of formation, Is proportional to the difference between the fugacity of the unresolved gas and the equilibrium three phases of the fugacity at laboratory temperature. This difference defines the driving force of the unification of the pressure effects. Speed constant indicates low temperature dependence [18].

Marzieh Zare et al. [2019] evaluated the effect of imidazolium based on ionic solutions and ethylene glycol monoethyl ether solution on the formation kinetics of methane hydrate. In the high-pressure reactor, methane hydration formation experiments were performed in the presence of imidazolium changes based on anionic liquid solutions with a concentration of 0.5. Induction time, gas consumption and temperature were measured. In addition, methane hydrate formation tests in the presence of ethylene glycol monoethyl ether (EGME) act as an inhibitor.

The simultaneous effect of ionic solution EGME on the formation of methane hydrate was investigated, so the effect of these substances depends on the type of ionic liquid and the concentration of EGME. The results revealed that the use of EGME with a concentration of 0.75 mol% in the presence of [BMIM] [MeSO4] and [OH-EMIM] [BF4] can improve the formation of methane hydrate. In contrast, these systems with EGME with concentration of 10% molar can function as a kinetic inhibitor in the formation of methane hydrate [9].

Model Harry et al

Harry [41] investigated the mechanism of crystallization of methane hydrate using particle size distribution. First, in the experimental part of the research, based on the measurement of turbidity, the particle size distribution solution was formed to form methane hydrate, and then the particle population density was calculated. Then, after sufficient time, the average particle size and the total number of particles were determined and a model was presented to justify the particle behavior. In fact, the study sought to

investigate the effect of agitator speed on changes in average particle size and total number of particles over time. The effect of agitator speed on the average size and total number of particles during the crystallization of methane hydrate at a pressure of 30 bar and a temperature of 1 °C has been investigated.

At low agitator speeds (250 rpm) the average particle size increases with time but at high agitator speeds (600 rpm) the average particle size decreases. In the case of the total number of particles, the opposite is true, and at low agitator speeds the increase in the total number of particles with time is negligible, but at high agitator speeds the increase in the number of particles with time is much more severe. Harry et al. Attempted to develop the following model to explain the complex effect of agitator speed on particle size distribution. By measuring the turbidity of the solution, the particle size distribution was obtained and the particle abundance equilibrium equation was used:

$$\frac{\partial \varphi}{\partial t} + G\frac{\partial \varphi}{\partial r} = \left(B_{I.1} + B_{I,2}\right)\delta(r)$$

In this regard, $\varphi(r,t)$ the population density of particles has radius r and time t. G is the $\left(\frac{dr}{dt}\right)$ growth rate. $\delta(r)$ It is a function of the delta whose value is zero at time zero, which means that the particles formed by primary nucleation have an initial size of zero. Terms $B_{I,1}$ and $B_{I,2}$ respectively are the secondary nucleation rate in the film region and the primary nucleation rate in the liquid mass (number of nuclei formed per unit volume and time).

hydrate former in a completely transparent reactor. They observed that the concentration of SDS 3-10 was sufficient to prevent the correlation of hydrate particles and the formation of a hard hydrate layer at the liquid-gas interface, and in the presence of SDS, more hydrates grew on the reactor wall as a porous structure. It is soluble due to capillary force. Hydrates grow in large quantities and up to 97% of the water in the reactor is converted to hydrates.

Conclusion

The highest decomposition temperature of the mixture of hydrate crystals is 0.1 MPa and the temperature of 285 K5 for xTBAB = 0.2 is the molar component of TBAB (TBAB + TBAC), which in comparison with pure hydrate is in Temperature K (285.5 and 288.2) and is higher for TBAB and TBAC hydrates. In addition, the enthalpies of formation of mixed hydrates in comparison with the resulting hydrates (5.55 ± 0.06) kJ.mol-1H2O} for pure hydrate TBAB and 0.05) KJ.mol-1H2O (5/30% for pure hydrate TBAC} more, and with maximum (5.95 ± 0.12) kJ. MoL -1 H2O to some extent 4/0 = xTBAB is registered.

Gait et al examined the in vitro determination of the decomposition curve of methane hydrate up to MPa55 pressure using a small amount of surface activator as an enhancer. 275) was studied and this temperature range is related to MPa pressure equilibrium (15-55.5). Testing the formation or decomposition of hydrates in a high-pressure reactor under isocuric conditions (a process that keeps the system volume constant) and was done without stirring.

A small amount of surfactant (molar concentration of 0.02% sodium dosyl sulfate) was added to the water to improve hydrate formation. It was estimated that SDS had no effect on the gas-to-hydrate balance and the amount of water converted to hydrate, both of which increased sharply when compared to experiments without surface activators. To understand and clarify the effect of SDS on hydrate formation, microscopic observations of hydrate growth were made by propane gas as a

Hamid Khorsand and Nasim Kiai evaluated the conditions for the formation of gas hydrates in the presence of thermodynamic improvers and inhibitors. In this study, the conditions of gas hydrate formation in the presence of thermodynamic improvers and inhibitors were investigated.

Also, thermodynamic models of gas hydrate formation in the presence of inhibitors are presented. The results showed that ionic liquids and other kinetic improvements accelerated the

formation of gaseous hydrates by reducing the surface tension of water. On the other hand, ionic liquids, salts and alcohols acted as thermodynamic inhibitors and caused the formation temperature of gaseous hydrates decreases.

Hossein Parhizgar et al. New Model for Predicting the Formation of Semi-Clarite Hydrate of Tetra Butyl Ammonium Bromide in the Presence of Methane, Carbon Dioxide and Nitrogen, Tetra Butyl Ammonium Chloride in the Presence of Methane and Carbon Dioxide and Tetra Butyl Ammonium Fluoride Carbon monoxide is treated. The results indicate that the formation of semi-clathrate hydrates has increased the potential of industrial applications of this type of hydrate. In this research, using van der Waals Plato theory, the activity coefficient equation of Thiers and Mayorga predicts the formation conditions of TBB salt in the presence of methane, carbon dioxide and nitrogen, TBAC salt in the presence of methane, carbon dioxide, carbon salt in the presence of TBAF.

Orcid

Alireza Bozorgian:

https://orcid.org/0000-0002-2454-5027

References

[1] C. Argentino, S. Conti, C. Fioroni, D. Fontana, *Geosciences*, **2019**, *9*, 134. **[crossref], [Google Scholar], [Publisher]**

[2] V.C. Nair, S.K. Prasad, R. Kumar, J.S. Sangwai, *Applied energy*, **2018**, *225*, 755-768. **[crossref], [Google Scholar], [Publisher]**

[3] Y. Wang, K. Yin, S. Fan, X. Lang, C. Yu, S. Wang, S. Li, *Energy*, **2021**, *217*, 119406. **[crossref], [Google Scholar], [Publisher]**

[4] A. Bozorgian, Z. Arab Aboosadi, A. Mohammadi, B. Honarvar, A. Azimi, *Eurasian Chem. Commun.*, **2020**, *2*, 420-426. **[crossref], [Google Scholar], [Publisher]**

[5] S. Wang, J. Xu, S. Fan, Y. Wang, X. Lang, C. Yu, *Fuel*, **2021**, *293*, 120482. **[crossref], [Google Scholar], [Publisher]**

[6] G. Li, S. Ma, F. Ye, L. Zhou, Y. Wang, X. Lang, S. Fan, *Industrial & Engineering Chemistry Research*, **2021**, *60*, 1799-1807. **[crossref], [Google Scholar], [Publisher]**

[7] S. Fan, H. Zhang, G. Yang, Y. Wang, G. Li, X. Lang, *Energy & Fuels*, **2020**, *34*, 13566-13579. **[crossref], [Google Scholar], [Publisher]**

[8] A. Bozorgian, *J. Chem. Rev.*, **2021**, *3*, 50-65. **[crossref], [Google Scholar], [Publisher]**

[9] Q. Ouyang, S. Fan, Y. Wang, X. Lang, S. Wang, Y. Zhang, C. Yu, *Energy & Fuels*, **2020**, *34*, 12476-12485. **[crossref], [Google Scholar], [Publisher]**

[10] S. M. S. Mirnezami, F. Zare Kazemabadi, A. Heydarinasab, *Progress in Chemical and Biochemical Research,* **2021**, 4, 191-206. **[crossref], [Google Scholar], [Publisher]**

[11] Y. Bi, T. Li, *The Journal of Physical Chemistry*, **2014**, *118*, 13324-13332. **[crossref], [Google Scholar], [Publisher]**

[12] M. Bagheri Sadr, A. Bozorgian, *J. Chem. Rev.*, **2021**, *3*, 66-82. **[crossref], [Google Scholar], [Publisher]**

[13] A. Bozorgian, *Adv. J. Chem. B*, **2021**, *3*, 54-61. **[crossref], [Google Scholar], [Publisher]**

[15] B. Wang, H. Dong, Y. Liu, X. Lv, Y. Liu, J. Zhao, Y. Song, *Appl. En- ergy*, **2018**, *227*, 710–718. **[crossref], [Google Scholar], [Publisher]**

[16] J.F. Zhao, D. Liu, M.J. Yang, Y.C. Song, *Int. J. Heat Mass Transf.*, **2014**, *77*, 529–541. **[crossref], [Google Scholar], [Publisher]**

[17] A. Bozorgian, A. Samimi, *Int. J. New Chem.*, **2021**, *8*, 41-58. **[crossref], [Google Scholar], [Publisher]**

[18] F. Zare Kazemabadi, A. Heydarinasab, A. Akbarzadehkhiyavi, M. Ardjmand, *Chemical Methodologies,* **2021**, 5, 135-152. **[crossref], [Google Scholar], [Publisher]**

[19] B. Wang, H. Dong, Z. Fan, J. Zhao, Y. Song, *Energy Procedia*, **2017**, *105*, 4713–4717. **[crossref], [Google Scholar], [Publisher]**

[20] S.R. Xu, S.S. Fan, H.Y. Yao, Y.H. Wang, X.M. Lang, P.P. Lv, S.T. Fang, *J. Chem. Thermodyn.*, **2017**, *104*, 212–217. **[crossref], [Google Scholar], [Publisher]**

[21] A. Bozorgian, *J. Eng. Indu. Res.*, **2020**, *1*, 1-19. **[crossref], [Google Scholar], [Publisher]**

[22] M. Li, S. Fan, Y. Su, J. Ezekiel, M. Lu, L. Zhang, *Energy*, **2015**, *90*, 202-207. **[crossref], [Google Scholar], [Publisher]**

[23] L. Zhang, Y. Kuang, X. Zhang, Y. Song, Y. Liu, J. Zhao, *Ind. Eng. Chem. Res.*, **2017**, *56*, 7585–

7592. [crossref], [Google Scholar], [Publisher]
[24] H. Kim, W. Yoo, Y. Lim, Y. Seo, *J. Pet. Sci. Eng.*, **2018**, *164*, 417–426. [crossref], [Google Scholar], [Publisher]
[25] M. Bagheri sadr, A. Bozorgian, *Int. J. Adv. Stu. Hum. Soc. Sci.*, **2020**, *9*, 252-261. [crossref], [Google Scholar], [Publisher]
[26] F. Zare Kazemabadi, A. Heydarinasab, A. Akbarzadeh, M. Ardjmand, *Artificial cells, nanomedicine, and biotechnology,* **2019**, 47, 3222-3230. [crossref], [Google Scholar], [Publisher]
[27] K. Li, R. Shi, Y. Huang, L. Tang, X. Cao, Y. Su, J. Zhao, *Computational and Theoretical Chemistry* ,**2018**, *1123*, 79–86. [crossref], [Google Scholar], [Publisher]
[28] G. Song, Y. Li, W. Wang, K. Jiang, Z. Shi, X. Ye, P. Zhao, *Journal of Natural Gas Science and Engineering* ,**2017**,*45*, 26–37. [crossref], [Google Scholar], [Publisher]
[29] A. Bozorgian, *Int. J. Adv. Stu. Hum. Soc. Sci.*, **2020**, *9*, 241-251. [crossref], [Google Scholar], [Publisher]
[30] N. Kayedi, A. Samimi, M. Asgari Bajgirani, A. Bozorgian, *South African Journal of Chemical Engineering*, **2021**, *35*, 153-158. [crossref], [Google Scholar], [Publisher]
[31]. A. Saberi, A. Alamdari, A. Shariati, A.H. Mohammadi, *Fluid Phase Equilibria*, **2018**, *459*, 110-118. [crossref], [Google Scholar], [Publisher]
[32] M. Aminnaji, B. Tohidi, R. Burgass, M. Atilhan, *Journal of Natural Gas Science and Engineering*, **2017**, *40*, 17–23. [crossref], [Google Scholar], [Publisher]
[33] J. Du, X. Wang, H. Liu, P. Guo, Z. Wang, S. Fan, *Fluid Phase Equilib.,* **2019**, *479*, 1–8. [crossref], [Google Scholar], [Publisher]
[47] J. Javanmardi, S. Babaee, A. Eslamimanesh, A.H. Mohammadi, *Journal of Chemical and Engineering Data*, ,**2012**, *57*, 1474–1479. [crossref], [Google Scholar], [Publisher]
[48] M.D. Jager, E.D. Sloan, *Fluid Phase Equilib*. **2001**, *185*, 89–99. [crossref], [Google Scholar], [Publisher]
[49] H. Haghighi, A. Chapoy, R. Burgess, S. Mazloum, B. Tohidi, *Fluid Phase Equilib*. **2009**, *278*, 109–116. [crossref], [Google Scholar], [Publisher]
[34] A. Bozorgian, *Int. J. Adv. Stu. Hum. Soc. Sci.*, **2020**, *9*, 229-240. [crossref], [Google Scholar], [Publisher]
[35] Q.N. Lv, X.R. Zang, X.S. Li, G. Li, *Fluid Phase Equilib.*, **2018**, *458*, 272–277. [crossref], [Google Scholar], [Publisher]
[36] S.R. Xu, S.S. Fan, Y.H. Wang, X.M. Lang, *Chem. Eng. Sci.*, **2017**, *171*, 293–302. [crossref], [Google Scholar], [Publisher]
[37] J. Park, K.C. da Silveira, Q. Sheng, C.D. Wood, Y. Seo, *Energy Fuel*, **2017**, *31*, 2697–2704. [crossref], [Google Scholar], [Publisher]
[38] A. Bozorgian, *Int. J. Adv. Stu. Hum. Soc. Sci.*, **2020**, *9*, 205-218. [crossref], [Google Scholar], [Publisher]
[39] Z.R. Chong, J.W. Koh, P. Linga, *Energy*, **2017**, *137*, 518–529. [crossref], [Google Scholar], [Publisher]
[40] J. Mashhadizadeh, A. Bozorgian, A. Azimi, *Eurasian Chem. Commun.*, **2020**, *2*, 536-547. [crossref], [Google Scholar], [Publisher]
[41] N.N. Nguyen, A.V. Nguyen, *Energy Fuel*., **2017**, *31*, 10311–10323. [crossref], [Google Scholar], [Publisher]
[42] Y. Hu, B.R. Lee, A.K. Sum, *Journal of Natural Gas Science and Engineering*, **2017**, *46*, 750–755. [crossref], [Google Scholar], [Publisher]
[43] A.H. Mohammadi, D. Richon, *J. Chem. Eng. Data*, **2011**, *56*, 4544–4548. [crossref], [Google Scholar], [Publisher]
[45] H. Hashemi, S. Babaee, K. Tumba, AH. Mohammadi, P. Naidoo, *Petroleum Science and Technology*, **2019**, *37*, 506-512. [crossref], [Google Scholar], [Publisher]
[46] M. Aminnaji, B. Tohidi, R. Burgass, M. Atilhan, *Journal of Natural Gas Science and Engineering*, **2017**, *45*, 840–847. [crossref], [Google Scholar], [Publisher]
[50] A. Bozorgian, *Adv. J. Sci. Eng.*, **2020**, *1*, 34-39. [crossref], [Google Scholar], [Publisher]
[51] Y. Bi, A. Porras, T. Li, *The Journal of chemical physics*, **2016**, *145*, 211909. [crossref], [Google Scholar], [Publisher]
[52] S. Wang, S. Fan, X. Lang, Y. Wang, P. Wang, *Fuel*, **2020**, *259*, 116201. [crossref], [Google Scholar], [Publisher]
[53] S.E. Mousavi, A. Bozorgian, *Int. J. New Chem.*, **2020**, *7*, 195-219. [crossref], [Google Scholar], [Publisher]

[54] M.F. Sánchez-Mora, L.A. Galicia-Luna, A. Pimentel-Rodas, A.H. Mohammadi, *Journal of Chemical & Engineering Data*, **2019**, *64*, 763-770. [crossref], [Google Scholar], [Publisher]
[55] A. Bozorgian, S. Zarinabadi, A. Samimi, *J. Chem. Rev.*, **2020**, *2*, 122-129. [crossref], [Google Scholar], [Publisher]
[56] A. Samimi, S. Zarinabadi, A. Bozorgian, A. Amosoltani, *Prog. Chem. Biochem. Res.*, **2020**, *3*, 46-54. [crossref], [Google Scholar], [Publisher]
[57] S.P. Kang, J.Y. Shin, J.S. Lim, S. Lee, *Chem. Eng. Sci.*, **2014**, *116*, 817–823. [crossref], [Google Scholar], [Publisher]
[58] R. O'Reilly, N.S. Ieong, P.C. Chua, M.A. Kelland, *Chem. Eng. Sci.*, **2011**, *66*, 6555–6560. [crossref], [Google Scholar], [Publisher]
[59] R. O'Reilly, N.S. Ieong, P.C. Chua, M.A. Kelland, *Energy Fuel*, **2011**, *25*, 4595–4599. [crossref], [Google Scholar], [Publisher]
[60] M.F. Mady, M.A. Kelland, *Energy Fuel*, **2014**, *28*, 5714–5720. [crossref], [Google Scholar], [Publisher]
[61] A. Bozorgian, Z.A. Aboosadi, A. Mohammadi, B. Honarvar, A. Azimi, *J. Chem. Pet. Eng.*, **2020**, *54*, 73-81. [crossref], [Google Scholar], [Publisher]
[62] M. Shi, X. Lang, Y. Wang, N. Von Solms, S. Fan, *Energy & Fuels*, **2019**, *33*, 3473-3482. [crossref], [Google Scholar], [Publisher]
[63] F.T. Reyes, M.A. Kelland, *Energy Fuel*, **2013**, *27*, 3730–3735. [crossref], [Google Scholar], [Publisher]
[64] F.T. Reyes, M.A. Kelland, *Energy Fuel*, **2013**, *27*, 1314–1320. [crossref], [Google Scholar], [Publisher]
[65] F.T. Reyes, E.L. Malins, C.R. Becer, M.A. Kelland, *Energy Fuel*, **2013**, *27*, 3154–3160. [crossref], [Google Scholar], [Publisher]
[66] M.F. Mady, M.A. Kelland, *Energy Fuel*, **2015**, *29*, 678–685. [crossref], [Google Scholar], [Publisher]
[68] M.A. Kelland, E. Abrahamsen, H. Ajiro, M. Akashi, *Energy Fuel*, **2015**, *29*, 4941–4946. [crossref], [Google Scholar], [Publisher]
[69] F.T. Reyes, M.A. Kelland, N. Kumar, L. Jia, *Energy Fuel*, **2015**, *29*, 695–701. [crossref], [Google Scholar], [Publisher]
[70] C.D. Magnusson, D. Liu, E.Y.X. Chen, M.A. Kelland, *Energy Fuel*, **2015**, *29*, 2336–2341. [crossref], [Google Scholar], [Publisher]
[71] H.J. Huo, R.H. Wang, H.J. Ni, Y.L. Liu, *Pet. Sci. Technol.*, **2014**, *32*, 1940–1947. [crossref], [Google Scholar], [Publisher]
[72] E.F. May, R. Wu, M.A. Kelland, Z.M. Aman, K.A. Kozielski, P.G. Hartley, N. Maeda, *Chem. Eng. Sci.*, **2014**, *107*, 1–12. [crossref], [Google Scholar], [Publisher]
[74] M.A. Kelland, N. Moi, M. Howarth, *Energy Fuel*, **2013**, *27*, 711–716. [crossref], [Google Scholar], [Publisher]
[75] L.H.S. Ree, M.F. Mady, M.A. Kelland, *Energy Fuel*, **2015**, *29*, 7923–7930. [crossref], [Google Scholar], [Publisher]
[76] J. Du, X. Wang, H. Liu, P. Guo, Z. Wang, S. Fan, *Fluid Phase Equilibria*, **2019**, *479*, 1-8. [crossref], [Google Scholar], [Publisher]
[77] A. Bozorgian, *Adv. J. Chem. B*, **2020**, *2*, 91-101. [crossref], [Google Scholar], [Publisher]
[78] H. Yarveicy, M.M. Ghiasi, A.H. Mohammadi, *Chemical Engineering Research and Design*, **2018**, *132*, 208-214. [crossref], [Google Scholar], [Publisher]
[79] C.D. Magnusson, M.A. Kelland, *Energy Fuel*, **2014**, *28*, 6803–6810. [crossref], [Google Scholar], [Publisher]
[80] M.E. Mady, M.A. *Chem. Eng. Sci.*, **2016**, *144*, 275–282. [crossref], [Google Scholar], [Publisher]
[81] E.A. Mahdiraji, A. Yousefi Talouki, *Journal of Chemical Reviews*, **2020**, *2*, 284-291. [crossref], [Google Scholar], [Publisher]
[82] E.A. Mahdiraji, M.S. Amiri, *Journal of Engineering in Industrial Research*, **2020**, *1*, 111-122. [crossref], [Google Scholar], [Publisher]
[83] E.A. Mahdiraji, M.S. Amiri. *Journal of Engineering Technology and Applied Sciences*. **2020**, *5*, 133-147. [crossref], [Google Scholar], [Publisher]
[84] M.F. Mady, M.A. Kelland, *Energy Fuel*, **2018**, *32*, 4841–4849. [crossref], [Google Scholar], [Publisher]
[85] M.A. Kelland, A.H. Kvaestad, E.L. Astad, *Energy Fuel*, **2012**, *26*, 4454–4464. [crossref], [Google Scholar], [Publisher]

[86] A. Bozorgian, *Prog. Chem. Biochem. Res.*, **2020**, *3*, 169-179. **[crossref], [Google Scholar], [Publisher]**
[87] S.R. Xu, S.S. Fan, S.T. Fang, X.M. Lang, Y.H. Wang, J. Chen, *Sci. Rep.*, **2016**, *6*. **[crossref], [Google Scholar], [Publisher]**
[88] E.A. Mahdiraji, N. Ramezani, *2015 2nd International Conference on Knowledge-Based Engineering and Innovation (KBEI)*, Tehran, Iran, **2015**, 405-411. **[crossref], [Google Scholar], [Publisher]**
[89] C. Magnusson, E. Abrahamsen, M.A. Kelland, A. Cely, K. Kinnari, X. Li, K.M. Askvik, *Energy Fuel*, **2018**, *32*, 5772–5778. **[crossref], [Google Scholar], [Publisher]**
[90] A. Bozorgian, *Chem. Rev. Lett.*, **2020**, *3*, 94-97. **[crossref], [Google Scholar], [Publisher]**
[91] A. Samimi, K. Kavosi, S. Zarinabadi, A. Bozorgian, *Prog. Chem. Biochem. Res.*, **2020**, *3*, 7-19. **[crossref], [Google Scholar], [Publisher]**
[92] M.A. Kelland, Q. Zhang, P.C. Chua, *Energy Fuel*, **2018**, *32*, 9349–9357. **[crossref], [Google Scholar], [Publisher]**
[93] N. Maeda, M.A. Kelland, C.D. Wood, *Chem. Eng. Sci.*, **2018,** *183*, 30–36. **[crossref], [Google Scholar], [Publisher]**
[94] N.A. Mohamed, M. Tariq, M. Atilhan, M. Khraisheh, D. Rooney, G. Garcia, S. Aparicio, *J. Chem. Thermodyn.*, **2017**, *111*, 7–19. **[crossref], [Google Scholar], [Publisher]**
[95] L.L. Ree, M.A. Kelland, D. Haddleton, F. Alsubaie, *Energy Fuel*, **2017**, *31*, 1355–1361. **[crossref], [Google Scholar], [Publisher]**
[96] A. Bozorgian, S. Zarinabadi, A. Samimi, *Chem. Methodol.*, **2020**, *4*, 477-493. **[crossref], [Google Scholar], [Publisher]**
[97] E.A. Mahdiraji, M.S. Amiri. *International Journal of Smart Electrical Engineering*, **2020,** *9*, 13-21. **[crossref], [Google Scholar], [Publisher]**
[98] E.A. Mahdiraji, M. Amiri, *Journal of Engineering Technology and Applied Sciences*. **2020**, *5*, 133-147. **[crossref], [Google Scholar], [Publisher]**
[99] M.M.A. Aziz, E.S.T. El Din, D.K.L Ibrahim, M. Gilany, *Electric Power Components and Systems,* **2006**, *34*, 417–432. **[crossref], [Google Scholar], [Publisher]**
[100] A. Bozorgian, *Chem. Rev. Lett.*, **2020**, *3*, 79-85. **[crossref], [Google Scholar], [Publisher]**
[101] A. Bozorgian, Z. Arab Aboosadi, A. Mohammadi, B. Honarvar, A. Azimi, *Prog. Chem. Biochem. Res.*, **2020**, *3*, 31-38. **[crossref], [Google Scholar], [Publisher]**
[102] J.R. Hall, P.W. Baures, *Energy Fuel*, **2017**, *31*, 7816–7823. **[crossref], [Google Scholar], [Publisher]**

Dr. Alireza Bozorgian was born in Kashan, (Iran). He completed his BSc, MSc and Ph.D. Degree in Chemical Engineering. He currently works in Chemical Engineering at the Islamic Azad University of Mahshahr. His studies focused on Heat Transfer, Transport Phenomena, Nanotechnology and Gas Hydrate. He has published more than 30 papers